CP violation in $B_s^0 \to J/\psi\phi$ in the ATLAS experiment

Radek Novotny on behalf of the ATLAS collaboration[*]

Czech Technical University in Prague, Czech Republic

E-mail: radek.novotny@cern.ch

The measurement of the *CP*-violation and other physics parameters in the $B_s^0 \to J/\psi(\mu^+\mu^-)\phi(K^+K^-)$ channel using data collected by the ATLAS detector from 13 TeV pp collisions at the LHC with integrated luminosity of $80.5\,\text{fb}^{-1}$ is presented. In addition to the *CP*-violating phase ϕ_s and the width difference $\Delta\Gamma_s$ between the B_s^0 meson mass eigenstates, the average decay width Γ_s and the transversity amplitudes including corresponding strong phases are measured. The measured values are then combined with those from $19.2\,\text{fb}^{-1}$ of 7 TeV and 8 TeV data. All measurements are in agreement with the Standard Model predictions and other LHC measurements.

---

[*]Speaker.

1. Introduction

The $B_s^0 \to J/\psi\phi$ channel is used to measure the *CP*-violation phase ϕ_s which is potentially sensitive to New Physics (NP). In the $B_s^0 \to J/\psi\phi$ the *CP*-violation occurs due to interference between a direct decay and a decay with $B_s^0 - \bar{B}_s^0$ mixing. In the Standard Model (SM), ϕ_s is related to the CKM elements and is predicted with a high precision $\phi_s \simeq 2\arg[-(V_{ts}V_{tb}^*)/(V_{cs}V_{cb}^*)] = -0.0363^{+0.0016}_{-0.0015}$ rad [1]. The NP processes could introduce additional contributions to the box diagrams describing the B_s^0 mixing and change the predicted ϕ_s value. Although the large NP enhancements of the mixing amplitude have been excluded by the precise measurement of the oscillation frequency, there is still some room on the order of statistical uncertainty.

Other measured quantity in B_s^0 mixing is $\Delta\Gamma_s = \Gamma_s^L - \Gamma_s^H$, where Γ_s^L and Γ_s^H are the decay widths of the different mass eigenstates. The $\Delta\Gamma_s$ is not sensitive to NP, however the measurement is interesting for testing the SM prediction $\Delta\Gamma_s = 0.087 \pm 0.021$ ps^{-1} [2].

The analysis presented here introduces the measurement of the $B_s^0 \to J/\psi\phi$ decay parameters using 80.5 fb^{-1} of LHC [3] *pp* data collected by the ATLAS [4] detector during 2015–2017 at a centre-of-mass energy $\sqrt{s} = 13$ TeV [5]. The measured values are then combined with those from 19.2 fb^{-1} of 7 TeV and 8 TeV data [6].

2. The ATLAS detector

The ATLAS detector[4] is a multi-purpose purpose detector with a forward-backward symmetric cylindrical geometry and nearly 4π coverage in solid angle, designed for exploration of NP in *pp* collisions.

The ATLAS consists of subdetectors grouped into three groups. The first group of detectors called inner tracking detector (ID) consists of a silicon pixel detector, a silicon microstrip detector, and a transition radiation tracker. The inner detector is designed to provide an excellent momentum resolution for charged particles and both primary and secondary vertex position measurements with high precision in the pseudorapidity range of $|\eta| < 2.5$. It also provides electron identification over the region of $|\eta| < 2.0$. A new Insertable B-Layer [7] with a radius of 33 mm was installed between a new smaller beryllium beam pipe and the innermost pixel layer during Long Shutdown 1. The ID is surrounded by a thin superconducting solenoid providing a 2 T axial magnetic field, and by second group of detectors. The high-granularity liquid-argon (LAr) sampling electromagnetic calorimeter and a steel/scintillator tile calorimeter provide coverage in the central rapidity range. The end-cap and forward regions are instrumented with LAr calorimeters for electromagnetic and hadronic measurements. The last group of detectors is called muon spectrometer (MS) that surrounds the calorimeters and consists of three large superconducting toroids with eight coils each, a system of muon tracking chambers, and fast detectors for triggering on muon tracks.

3. Reconstruction and candidate selection

The events are collected with a mixture of triggers based on $J/\psi \to \mu^+\mu^-$ identification, with muon p_T thresholds of either 4 GeV or 6 GeV. Besides, each event must contain at least one reconstructed primary vertex, formed from at least four ID tracks, and at least one pair of oppositely charged muon candidates that are reconstructed using information from the MS and the ID. The pair of oppositely charged muon tracks is refitted to the common primary vertex and are accepted if $\chi^2/\text{ndf} < 10$. The candidates for the decay $\phi \to K^+K^-$ are reconstructed from all pairs of oppositely charged tracks, with $p_T > 1$ GeV and $|\eta| < 2.5$, that are not identified as muons. Candidate events for B_s^0 decays are selected by fitting the tracks for each combination of J/ψ and ϕ to a common vertex and is accepted if $\chi^2/\text{ndf} < 3$ and $1.0085\,\text{GeV} < m(K^+K) < 1.0305\,\text{GeV}$. The B_s^0 candidate with the lowest χ^2/ndf is selected in cases where more than one candidate passes all selections. In total, 3210429 B_s^0 candidates is collected within the mass range of $5150 - 5650\,\text{MeV}$. For each B_s^0 meson candidate the proper decay time t is estimated using:

$$t = \frac{L_{xy}\, m_B}{p_{T_B}}, \tag{3.1}$$

where p_{T_B} is the reconstructed transverse momentum of the B_s^0 meson candidate and m_B denotes the mass of the B_s^0 meson, taken from Ref. [8]. The transverse decay length, L_{xy}, is the displacement in the transverse plane of the B_s^0 meson decay vertex with respect to the primary vertex, projected onto the direction of the B_s^0 transverse momentum. The primary vertex position is recalculated after removing any tracks used in the B_s^0 meson candidate to avoid biasing L_{xy}.

4. Angular analysis and maximum likelihood fit

Because $B_s^0 \to J/\psi\phi$ is a pseudo-scalar to vector vector decay, the *CP*-odd (L=1) and *CP*-even (L=0,2) amplitudes are separated statistically through a full time-dependent angular analysis. For the description of the transversity angles, the rest frame of the decaying particles is used.

The decay amplitudes are decomposed using three independent linear polarization states A_0, $A_\perp$ and $A_\parallel$ of the vector mesons and are normalized such that $|A_0(0)|^2 + |A_\perp(0)|^2 + |A_\parallel(0)|^2 = 1$. For each of the transversity amplitudes there is an associated phase $\delta_0 = \arg(A_0)$, $\delta_\perp = \arg(A_\perp)$ and $\delta_\parallel = \arg(A_\parallel)$. However, the primary signal is diluted by other processes with the same final state such as non-resonant $B_s \to J/\psi K^+K^-$. These S-wave states have to be counted in the final description of the decay, using their own amplitude A_S and phase δ_S.

In order to extract physical parameters, the unbinned maximum likelihood fit to the B_s^0 candidates is performed. The fit uses information about the reconstructed mass m, the measured proper decay time t, the measured mass uncertainty σ_m, the measured proper decay time uncertainty σ_t, the tagging probability $P(B|Q_x)$, and the transversity angles $\Omega = (\theta_T, \psi_T, \phi_T)$ of each $B_s^0 \to J/\psi\phi$ decay candidate. The likelihood is defined as a combination of the signal Probability Density Function (PDF), combinatorial background PDF, distributions describing backgrounds from the $B_d^0 \to J/\psi K^{*0}$, $B_d^0 \to J/\psi K\pi$ and $\Lambda_b^0 \to J/\psi Kp$ misidentified as B_s^0 candidate and weighting factor to account for the trigger efficiency. The detailed description of the likelihood function and the systematic uncertainties can be found in Ref. [5].

5. Flavour tagging

To identify the initial flavour of the neutral B_s^0 meson, the opposite-side tagging is used. The opposite-side b-hadron is produced from the $b\bar{b}$ pair production in pp collisions. To identify initial flavour of the opposite b-hadron four types of taggers are used: two types of muons, electrons and when no lepton is found in the opposite side decay then b-jets. All methods are based on the same discriminating variable called *cone charge* which is defined as follows

$$Q_x = \frac{\sum_i^{N \text{ tracks}} q_i \cdot (p_{Ti})^\kappa}{\sum_i^{N \text{ tracks}} (p_{Ti})^\kappa}, \tag{5.1}$$

where $x = \{\mu, e, \text{jet}\}$ refers to muon, electron, or jet charge, respectively. The summation is made over a selected set of tracks in a cone, $\Delta R = \sqrt{(\Delta\phi)^2 + (\Delta\eta)^2} < 0.5$, around the lepton or jet direction. The constant κ is found empirically for each tagging method, respectively.

The calibration of each tagging method is using data containing $B^\pm \to J/\psi K^\pm$ candidate decays. The charge of the kaon in $B^\pm \to J/\psi K^\pm$ decay determines the initial flavour of the b-meson and gives us the cone charge probability distribution $P(Q_x|B^\pm)$. This probability is then used for the calculation of the probability to tag a B_s^0 meson containing a $\bar{b}$-quark as $P(B|Q_x) = P(Q_x|B^+)/(P(Q_x|B^+) + P(Q_x|B^-))$.

The performance of each tagging method is represented by tagging power defined as a $T_x = \sum_i \varepsilon_{xi} \cdot \mathscr{D}^2(Q_{xi})$, where the ε_x is the tag efficiency, and $\mathscr{D}(Q_x)$ is the dilution and the sum is over the probability distribution in intervals of the cone charge variable.

The efficiency, ε_x, of an individual tagging method is defined as the fraction of signal events tagged by that method compared to the total number of signal events in the sample. The dilution is defined as $\mathscr{D}(Q_x) = 2P(B|Q_x) - 1$ and represents the purity of a particular flavour tagging method. An effective dilution, $D_x = \sqrt{T_x/\varepsilon_x}$, is calculated from the measured tagging power and efficiency. The summary of tagging performance for each tagging method is given in Table 1.

Table 1: Summary of tagging performances on the sample of $B^\pm \to J/\psi K^\pm$ signal candidates for each tagging method. Taken from [5].

| Tag method	ε_x [%]	D_x [%]	T_x [%]
Tight muon	4.50 ± 0.01	43.8 ± 0.2	0.862 ± 0.009
Electron	1.57 ± 0.01	41.8 ± 0.2	0.274 ± 0.004
Low-pT muon	3.12 ± 0.01	29.9 ± 0.2	0.278 ± 0.006
Jet	5.54 ± 0.01	20.4 ± 0.1	0.231 ± 0.005
Total	14.74 ± 0.02	33.4 ± 0.1	$1.65 \ \pm 0.01$

6. Results

The simultaneous unbinned maximum-likelihood fit results with systematic uncertainties are shown in Table 2. These results are compatible with those obtained from ATLAS Run1 analysis using 19.2 fb^{-1} of 7 TeV and 8 TeV data [6]. The fit projections of the mass, proper decay time and angles are shown in Figure 1.

Table 2: Fitted values for the physical parameters of interest with their statistical and systematic uncertainties. Taken from [5].

	ϕ_s [rad]	$\Delta\Gamma_s$ [ps^{-1}]	Γ_s [ps^{-1}]	$|A_\parallel(0)|^2$	$|A_0(0)|^2$	$|A_S(0)|^2$	$\delta_\perp$ [rad]	$\delta_\parallel$ [rad]	$\delta_\perp - \delta_S$ [rad]
Value	-0.068	0.067	0.669	0.219	0.517	0.046	2.946	3.267	-0.220
Stat.	0.038	0.005	0.001	0.002	0.001	0.003	0.101	0.082	0.037
Syst.	0.018	0.002	0.001	0.002	0.004	0.004	0.097	0.201	0.010
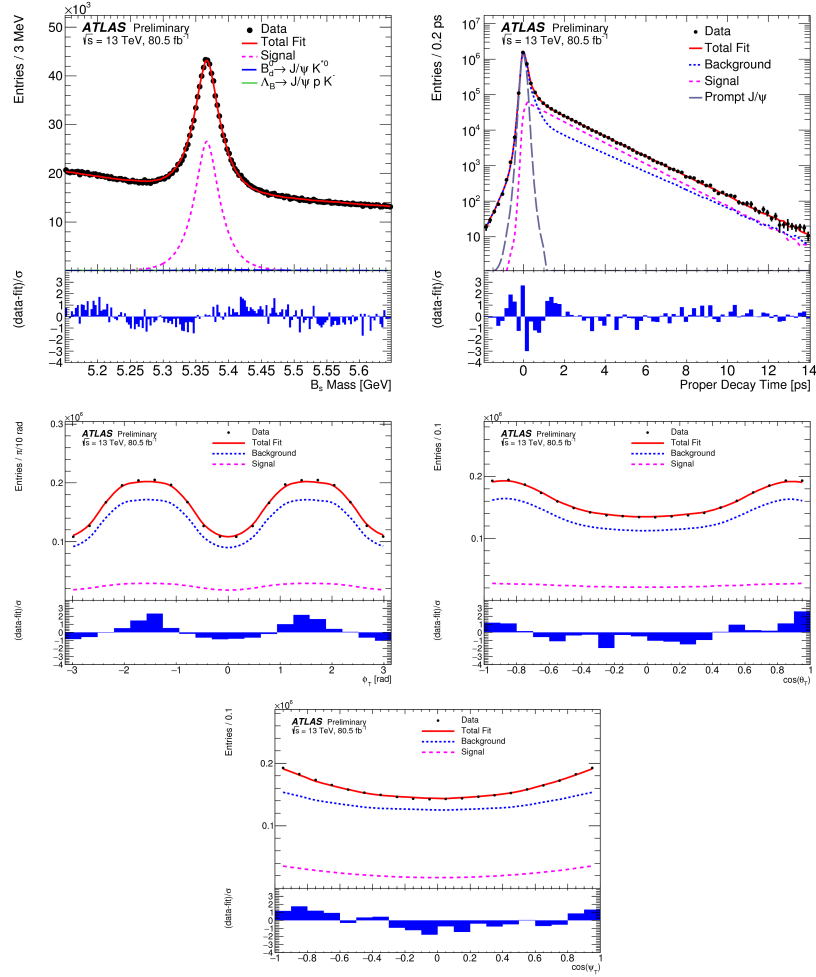
Figure 1: (top, left) Mass fit projection for the $B_s^0 \to J/\psi\phi$ sample. (top, right) Proper decay time fit projection for the $B_s^0 \to J/\psi\phi$ sample. Fit projections for the transversity angles ϕ_T (middle left), $\cos(\theta_T)$ (middle, right), and $\cos(\psi_T)$ (bottom). In all plots the red solid line shows the total fit, the $B_s^0 \to J/\psi\phi$ signal component is shown by the magenta dashed line and the blue dotted line shows the contribution of all background components. Below each figure is a ratio plot that shows the difference between each data point and the total fit line divided by the statistical and systematic uncertainties summed in quadrature (σ) of that point. Taken from [5].

The obtained parameters are combined with results from ATLAS Run1 measurements using a Best Linear Unbiased Estimator method (BLUE). This method uses the measured values and uncertainties of the parameters as well as the correlations between them. The combined values of parameters are shown in Table 3. The two dimensional contours in $\phi_s - \Delta\Gamma_s$ plane for both measurements and its combination is shown in Figure 2.

Table 3: Combined values for the physical parameters of interest with their statistical and systematic uncertainties. Taken from [5].

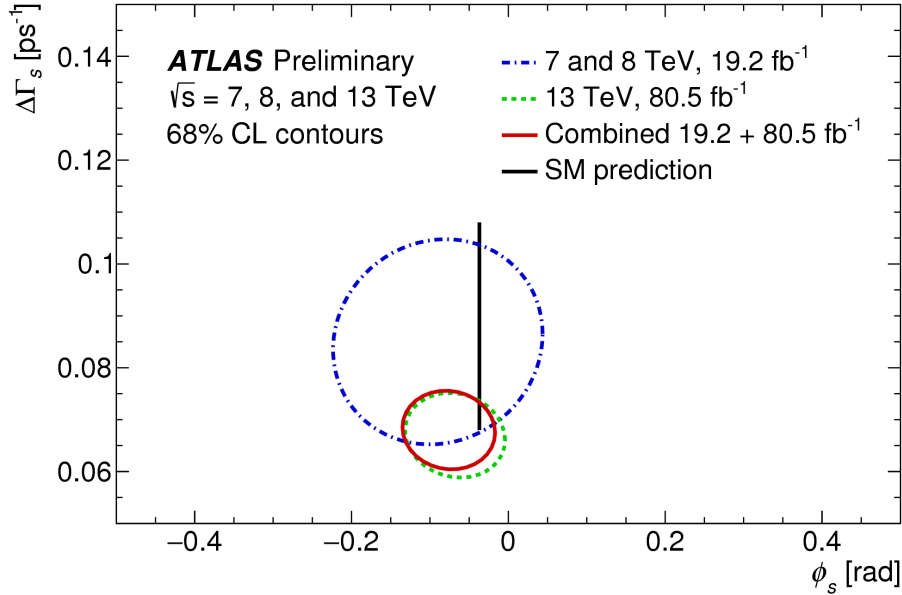|	ϕ_s [rad]	$\Delta\Gamma_s$ [ps^{-1}]	Γ_s [ps^{-1}]	$|A_\parallel(0)|^2$	$|A_0(0)|^2$	$|A_S(0)|^2$	$\delta_\perp$ [rad]	$\delta_\parallel$ [rad]	$\delta_\perp - \delta_S$ [rad]
Value	−0.076	0.068	0.669	0.220	0.517	0.043	3.075	3.295	−0.216
Stat.	0.034	0.004	0.001	0.002	0.001	0.004	0.096	0.079	0.037
Syst.	0.019	0.003	0.001	0.002	0.004	0.004	0.091	0.202	0.010

Figure 2: Likelihood 68% confidence level contours in the $\phi_s - \Delta\Gamma_s$ plane, showing ATLAS results for 7 TeV and 8 TeV data (blue dashed-dotted curve), for 13 TeV data (green dashed curve) and for 13 TeV data combined with 7 TeV and 8 TeV (red solid curve) data. In all contours the statistical and systematic uncertainties are combined in quadrature and correlations are taken into account. The Standard Model prediction is shown as a very thin black rectangle. Taken from [5].

7. Summary

A measurement of the time-dependent *CP* violation parameters in $B_s^0 \to J/\psi(\mu^+\mu^-)\phi(K^+K^-)$ decays from a 80.5 fb^{-1} data sample of *pp* collisions collected with the ATLAS detector during the 13 TeV LHC run is presented. The values from the 13 TeV analysis are consistent with those obtained in the previous analysis using 7 TeV and 8 TeV ATLAS data. The two measurements are statistically combined leading to the following results

$$\phi_s = -0.076 \pm 0.034(\text{stat.}) \pm 0.019(\text{syst.}) \text{ rad}$$
$$\Delta\Gamma_s = 0.068 \pm 0.004(\text{stat.}) \pm 0.003(\text{syst.}) \text{ ps}^{-1}$$
$$\Gamma_s = 0.669 \pm 0.001(\text{stat.}) \pm 0.001(\text{syst.}) \text{ ps}^{-1}$$

The new results from the ATLAS measurement on the *CP* violation phase ϕ_s in the $B_s^0 \to J/\psi\phi$ channel are consistent with Standard Model predictions as well as with other LHC measurements.

Acknowledgements

References

[1] J. Charles et al., *Predictions of selected flavour observables within the Standard Model*, Phys. Rev. **D84** (2011) 033005, arXiv: 1106.4041 [hep-ph].

[2] Alexander Lenz and Ulrich Nierste, *Numerical updates of lifetimes and mixing parameters of B mesons*, (2011), arXiv: 1102.4274 [hep-ph].

[3] Lyndon Evans and Philip Bryant, *LHC Machine*, JINST **3** (2008) S08001.

[4] ATLAS Collaboration, *The ATLAS Experiment at the CERN Large Hadron Collider*, JINST **3** (2008) S08003.

[5] ATLAS Collaboration, *Measurement of the CP violation phase ϕ_s in $B_s^0 \to J/\psi\phi$ decay in ATLAS at 13 TeV*, ATLAS-CONF-2019-009, 2019, URL: https://cds.cern.ch/record/2668482.

[6] ATLAS Collaboration, *Measurement of the CP-violating phase ϕ_s and the B_s^0 meson decay width difference with $B_s^0 \to J/\psi\phi$ decays in ATLAS*, JHEP **08** (2016) 147, arXiv: 1601.03297 [hep-ex].

[7] B. Abbott et al., *Production and integration of the ATLAS Insertable B-Layer*, JINST **13** (2018) T05008, arXiv: 1803.00844 [physics.ins-det].

[8] M. Tanabashi et al., *Review of Particle Physics*, Phys. Rev. **D98** (2018) 030001.